Journal of Alloys and Compounds, 187 (1992) 59–66
JALCOM 303

Raman and IR spectroscopy of hydrogen-charged $YBa_2Cu_3O_{7-\delta}$ films

A. Richter
Fachhochschule Ostfriesland, Constantiaplatz 4, W-2970 Emden (Germany)

G. Irmer
Fachbereich Physik, Bergakademie Freiberg, Bernhard-von-Cotta-Strasse 4,
O-9200 Freiberg (Germany)

G. Keßler and M. Panzner
Institut für Werkstoffphysik und Schichttechnologie der FhG, Helmholtzstr. 20,
O-8027 Dresden (Germany)

K. Herzog
Fachbereich Chemie, Technische Universität Dresden, Mommsenstrasse 13,
O-8027 Dresden (Germany)

(Received September 9, 1991; in final form February 19, 1992)

Abstract

Epitaxial superconducting Y $Ba_2Cu_3O_{7-\delta}$(YBCO) films have been deposited by laser ablation and charged with different amounts of hydrogen. At low hydrogen contents ($x \leqslant 0.5$) the hydrogen atoms are dissolved in the orthorhombic structure of YBCO without changes in the oxygen content. These hydrogen-charged YBCO films have been investigated by Raman and IR spectroscopy. Both experiments provide evidence that the charge carriers are strongly reduced by compensation with hydrogen. All five prominant Raman features of the orthorhombic YBCO system appear with modifications. The dominant 500 cm^{-1} Raman line is not shifted by hydrogen doping but decreases in intensity. Additional Raman modes are observed and attributed to disorder-induced modes.

1. Introduction

Superconducting properties of high T_c oxides are closely related to their structural characteristics. This finding has initiated the investigation of numerous chemical combinations in order to understand better the chemical role of the constituting elements and/or to improve the superconducting features. The effect of an additional light element such as hydrogen has been extensively studied [1–9]. A considerable effect of hydrogen atoms on the structural and physical properties governing superconductivity has been noticed in the $H_xYBa_2Cu_3O_{7-\delta}$ (H:YBCO) system.

It is well known that numerous metals and intermetallic compounds absorb hydrogen at relatively low temperatures [10]. The hydrogen atoms enter interstitial sites in order to form either dilute solid solutions or more

0925-8388/92/$5.00

concentrated hydride phases. In most cases, there is a significant change in the electronic structure due to the strong potential of the protons and the added electrons, resulting in a shift of the Fermi energy. This is of importance for the carrier concentration in the $YBa_2Cu_3O_{7-\delta}$ (YBCO) system as a sensitive factor for the electronic properties close to the metal–insulator transition.

A convenient way to change the carrier concentration in the YBCO material is to remove oxygen from the system. An alternative possibility is to replace yttrium by an element with a different valency, *e.g.* by praseodymium [11]. Hydrogen doping reduces the carrier concentration in YBCO as well [7, 8]. The normal-state resistivity increases monotonically with increasing hydrogen concentration. YBCO films charged with hydrogen remain superconducting up to $x = 0.4$ with a slightly lower superconducting transition temperature [9]. The T_c onset for undoped YBCO films on $SrTiO_3$ (100) or yttria-stabilized ZrO_2 substrates was at 90.5 K, with zero resistance at 89.5 K [12–15]. Hydrogen doping decreases the T_c onset temperature slightly to about 86 K but remains nearly constant with varying hydrogen concentration up to $x = 0.3$. However, the transition interval to zero resistance is drastically enlarged with 3.5 K and 7.2 K for $x = 0.1$ and $x = 0.25$ respectively [8, 9].

The site of the hydrogen atom in the YBCO unit cell and the character of the chemical bonds are not yet clear with certainty. Raman and IR techniques leave the basic chemical composition and the oxygen content of the YBCO superconducting material unchanged (see for example refs. 2 and 16–21). They are appropriate techniques for investigating H:YBCO films. Raman studies have provided insight into lattice dynamics and their variation with oxygen content and temperature and have given evidence for the superconducting gap. In the present paper we report on Raman and IR spectroscopy studies of H:YBCO films with different amounts of hydrogen.

2. Experimental details

Superconducting YBCO films were prepared by laser ablation from dense stoichiometric 1:2:3 targets with an XeCl excimer laser of wavelength 308 nm, pulse duration 20 ns and repetition rate 50 Hz [12–15]. The energy density at the rotating target was 1.7–4 J cm^{-2}. Films were deposited in flowing oxygen at a partial pressure of 40–80 Pa and substrate temperatures $T_s = 750$–845 °C. Deposition rates of 0.04 nm per pulse were estimated from the film thickness. Different conventional substrate materials such as $SrTiO_3$ (100), MgO (100), yttria-stabilized ZrO_2 and Si(100) wafers were used for sample preparation. Post-annealing was not necessary, since epitaxial superconducting films were grown by a definite slow-cooling procedure down to room temperature with increasing oxygen pressure within the deposition chamber after laser plasma deposition of the film. YBCO films of 600–800 nm thickness on $SrTiO_3$ substrates have been prepared to perform Raman measurements, whereas films 400 nm thick on MgO substrates have been used to obtain IR transmittance data.

The structures, morphologies and chemical compositions of the YBCO films prepared by the above-described *in situ* growth process have been investigated by X-ray diffraction, scanning electron microscopy, Rutherford backscattering spectroscopy and Auger electron spectroscopy analysis, and chemical methods such as multicomponent spectrophotometry and coulometry [18–21]. These measurements provide evidence for homogeneous epitaxial superconducting $YBa_2Cu_3O_{7-\delta}$ films with 1:2:3 stoichiometry and an oxygen content close to the ideal composition of seven oxygen atoms per orthorhombic unit cell. Deviations from this composition in the oxygen content are smaller than $\delta \leqslant 0.2$ and depend on temperature treatment and oxygen pressure.

Hydrogen charging was performed in a small ultrahigh vacuum chamber filled with pure hydrogen at a pressure slightly above 1 bar [9]. The YBCO films were carefully heated up to moderate temperatures of 130–150 °C in a hydrogen atmosphere. The hydrogen uptake took several hours depending on the desired hydrogen concentration in the films and was monitored by *in situ* resistivity measurements. Hydrogen depth profiles obtained with the ^{15}N nuclear reaction method show an increased hydrogen concentration near the film surface and a uniform hydrogen concentration after approximately 100 nm [9].

Raman measurements were carried out with an Ar^+ laser operating at wavelengths of 488 and 514.5 nm at a power density of 50 mW. The spectra were recorded at room temperature. In order to reduce thermal effects on the sample surface, the laser beam was defocused by optical elements. The frequency and intensity of the Raman modes were not affected by different laser wavelength excitations. Films have been investigated at various lateral positions without any noticeable changes in the Raman spectra, reflecting again the homogeneity of the H:YBCO films. IR transmission and reflection measurements of H:YBCO films were obtained with a Nicolet 320 Fourier transform spectrometer at room temperature purged by nitrogen gas in the wavenumber range 1000–4800 cm^{-1}.

3. Results and discussion

The Raman spectra of H:YBCO films charged with different amounts of hydrogen are represented in Fig. 1. Five characteristic Raman features have been observed at 500, 435, 340, 154 and 120 cm^{-1} for YBCO films without hydrogen (curve (a)), similar to those obtained by many workers [17–21]. Reliable assignments of the Raman modes to vibrational properties of the atoms in the YBCO unit cell were possible from polarization studies in combination with lattice dynamics calculations. Using the notation of Siegrist *et al.* [22] for the atoms in the YBCO unit cell, the observed Raman modes are assigned in the following manner [18]: axial motion of the O(1) atoms corresponds to the 500 cm^{-1} feature, Cu(2)–O(2) and Cu(2)–O(3) bond bending with O(2) and O(3) atoms moving in phase is related to the 435 cm^{-1} mode, Cu(2)–O(2) and Cu(2)–O(3) bond bending with the O(2) and

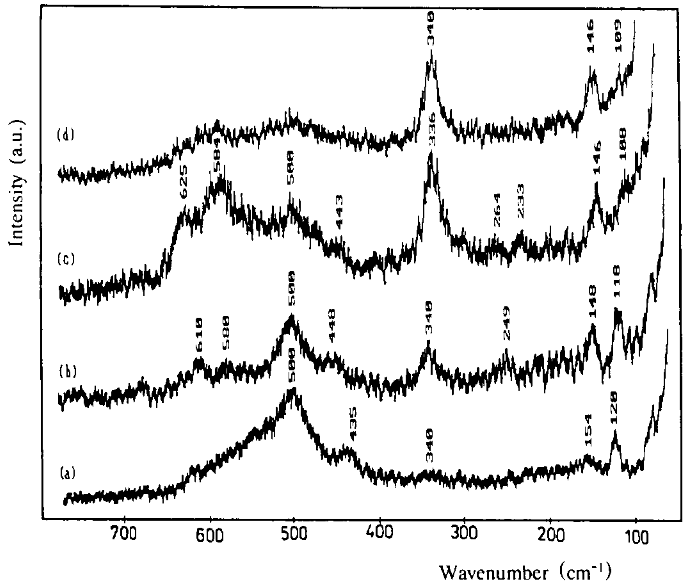

Fig. 1. Raman spectra of YBCO films charged with different hydrogen contents (a.u., arbitrary units): curve (a), $x=0$; curve (b), $x=0.1$; curve (c), $x=0.25$; curve (d), $x=0.5$.

O(3) atoms moving out of phase corresponds to the 340 cm^{-1} feature, and axial stretching of the Cu(2) atoms and barium atoms are related to the 154 cm^{-1} and 120 cm^{-1} modes respectively. These modes of the orthorhombic YBCO structure are of A_g symmetry. The Raman spectrum is dominated by oxygen vibrations which are of special interest. A continuous frequency and intensity variation for all five modes is observed, as the oxygen content varies. The intensity of the 500 cm^{-1} mode depends strongly on the oxygen concentration and becomes weak as the oxygen content decreases. The frequency shift was used as a measure for the oxygen content of the samples [17, 21]. Moreover, the large frequency shifts of the 500 cm^{-1} mode correspond to changes in the Cu(1)–Cu(2) distance along the *c* axis [18].

Hydrogen charging of the YBCO films does not cause a frequency shift of the 500 cm^{-1} line in the Raman spectra (Fig. 1). This seems to be evidence that the oxygen content of the films is not reduced by hydrogen doping. Further, it seems highly unlikely that hydrogen atoms are located near the O(1) atoms along the *c* axis, since no frequency shift of that feature is observed, which corresponds to changes in the Cu(1)–Cu(2) distance along the *c* axis. With increasing hydrogen content the intensity of this peak decreases drastically. For large hydrogen concentrations ($x \geqslant 0.5$), changes in the orthorhombic structure may occur, because the dominant 500 cm^{-1} Raman mode disappears.

Hydrogen doping modifies the observed Raman spectra of pure YBCO films. New peaks appear; others are shifted in frequency and/or changed in intensity. We assign the multiplicity in the Raman spectra to changes in the carrier concentration near the Fermi energy. The dissolved hydrogen in the

YBCO unit cell donates electrons to the conduction band and thereby compensates the hole charge carrier. This decreases the electronic shielding and therefore causes an increased intensity of existing modes and the appearance of additional modes.

There is an intense enhancement of the 340 and 154 cm^{-1} Raman lines with increasing hydrogen content. The 154 cm^{-1} mode is slightly shifted to lower wavenumbers. These two peaks even dominate in the spectra for the large hydrogen concentration $x = 0.5$. The 120 cm^{-1} barium vibration mode becomes soft and decreases in intensity with high hydrogen charging. The 435 cm^{-1} feature hardens and decreases in intensity with increasing hydrogen concentration and disappears for $x = 0.5$.

Raman investigations of YBCO samples with different oxygen contents show a dominant shift of the 500 cm^{-1} Raman frequency to lower wavenumbers for oxygen deficiency. Beside this, both the 340 and the 435 cm^{-1} lines have a dependence on δ opposite to the 500 cm^{-1} feature [17]. Our measurements deviate from this behaviour. The 500 and 340 cm^{-1} peaks are not shifted in frequency. The hardening of the 435 cm^{-1} mode and the softening of the 154 cm^{-1} mode are very similar to findings in investigations of YBCO samples with decreasing oxygen content. Because the main changes in Raman spectra of oxygen-deficient YBCO samples are not observed in our H:YBCO films, hydrogen causes effects other than oxygen deficiency. Hadjiev *et al.* [7] even found a hardening of the 500 cm^{-1} mode for hydrogenated samples.

Distinct peaks have been observed at 233, 249, 264, 584, 610 and 625 cm^{-1} for H:YBCO films which we attribute to the disturbed orthorhombic structure of YBCO. Two of these features at 248 and 610 cm^{-1} were investigated by Hadjiev *et al.* [7] as well as the 210 cm^{-1} line which we have not found. For $x = 0.5$ these additional lines disappear, indicating basic changes in the chemical composition and structure. Additional Raman modes of YBCO samples without hydrogen are observed at 220 and 580 cm^{-1} and in the region 550–650 cm^{-1} [21]. They are assigned to Raman-forbidden modes which have become Raman active owing to disorder induced by oxygen vacancies, defects or twinning. It is reasonable to assume that the Raman scattering selection rules break down for those forbidden modes which involve mainly vibrations of hydrogen nearest neighbours. Increasing disorder in the CuO chains caused by hydrogen atoms close to Cu(1) and O(4) sites could be the origin for the activation of the Cu(1)–O(4) stretching mode at around 580 cm^{-1}.

Raman data on $YBa_2Cu_4O_{8-\delta}$ [23] show two strong modes with frequencies of 257 and 600 cm^{-1} which do not exist in the 1:2:3 YBCO samples. The 600 cm^{-1} line is associated with the O–Cu axial stretching A_g mode of Cu(3)–O(4) and Cu(1)–O(5), whereas the 257 cm^{-1} line is caused by Cu(1) and Cu(3) atoms moving out of phase. It is tempting to assign the lines at 249, 269 and 610 cm^{-1} in H:YBCO films to modes of again Cu(1)–O(4) and Cu(1). Other planar Cu–O modes at wavenumbers above 600 cm^{-1} become Raman active when the symmetry of the structure is lowered, *e.g.*

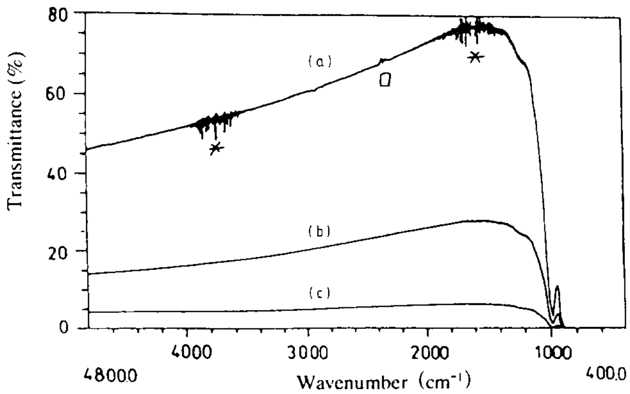

Fig. 2. IR transmittance spectra for an MgO(100) substrate without device cleaning with flowing nitrogen (curve (a)), for a YBCO film without hydrogen (curve (b)) and for a H:YBCO film with a hydrogen content $x=0.2$ (curve (c)); water (*) and CO_2 (□) absorption bands are marked.

by oxygen vacancies on O(4) sites [21]. Hydrogen atoms close to the vibrating atoms may result in similar effects. Since hydrogen atoms violate the Raman scattering selection rules, resulting in the appearance of additional modes, hydrogen seems to occupy preferentially the interstitial sites around Cu(1) and O(4).

IR transmittance data are shown in Fig. 2. The region of H_2O and CO_2 absorption bands is marked for comparison on the curve obtained from measurements on MgO substrates without purging the device with dry flowing nitrogen. This shows the necessity of excluding atmospheric conditions, since traces of water vapour and CO_2 on the MgO surface are indicated in the spectra. The superconducting YBCO film is characterized by a very low transmittance in the wavenumber range 1100–4000 cm^{-1} without additional resonances. The transmittance increases with hydrogen charging, indicating a reduction in the number of free charge carriers. This provides further evidence that hydrogen charging acts as compensation centre for charge carriers in H:YBCO. Additional absorption bands, especially O–H bonds with resonances in the range 3100–3700 cm^{-1}, have not been found, in agreement with the results of Yang *et al.* [2]. It is, however, not clear whether the film thickness is sufficient to analyse O–H bonds. IR spectroscopy studies on a fine and homogeneous YBCO powder charged with hydrogen are under investigation and the results will be published in a forthcoming paper. In this case, IR studies on YBCO powder always indicate an absorption peak at 1467 cm^{-1} which we attribute to carbon compound vibrations instead of to Cu–H stretching modes as discussed in ref. 2.

4. Conclusion

In conclusion, we have presented Raman and IR spectra of H:YBCO films with different hydrogen concentrations. At low hydrogen charging the hydrogen atoms are dissolved in the orthorhombic structure of the YBCO. The oxygen content is not changed by hydrogen doping. Hydrogen charging acts as compensation centres for charge carriers and decreases the hole carrier concentration in YBCO. Additional Raman modes to the commonly observed five peaks of A_g symmetry are attributed to disorder-induced modes in the orthorhombic system. Hydrogen seems to occupy preferentially interstitial sites around Cu(1) and O(4) atoms. For large hydrogen concentrations $x \geqslant 0.5$, chemical and structural changes are indicated in the Raman spectra.

Acknowledgments

The authors are indebted to A. Weidinger, J. Erxmeyer and B. Mertesacker, Hahn-Meitner-Institut, Berlin, for permanent support, hydrogen charging of the YBCO films and numerous discussions in the course of this work.

References

1 J. J. Reilly, M. Suenaga, J. R. Johnson, P. Thompson and A. R. Moodenbaugh, *Phys. Rev. B, 36* (1987) 5694.

2 C. Y. Yang, X.-Q. Yang, S. M. Heald, J. J. Reilly, T. Skotheim, A. R. Moodenbaugh and M. Suenaga, *Phys. Rev. B, 36* (1987) 8798.

3 M. Nicolas, J. N. Daou, I. Vedel, P. Vajda, J. P. Burger, J. Lesueur and L. Dumoulin, *Solid State Commun., 66* (1988) 1157.

4 H. Fujii, H. Kawanaka, W. Ye, S. Orimo and H. Fukuba, *Jpn. J. Appl. Phys., 27* (1988) L525.

5 Ch. Niedermayer, H. Glückler, R. Simon, A. Golnik, M. Rauer, E. Recknagel, A. Weidinger, J. I. Budnick, W. Paulus and R. Schöllhorn, *Phys. Rev. B, 40* (1989) 11386.

6 D. Fruchart, J. L. Soubeyroux, D. Tran Qui, C. Pique, C. Rillo, F. Lera, V. Orera, J. Flokstra and D. H. A. Blank, *J. Less-Common Met., 157* (1990) 233.

7 V. G. Hadjiev, M. V. Abrashev, M. N. Iliev and L. N. Bozukov, *Physica C, 171* (1990) 257.

8 H. Glückler, Ch. Niedermayer, G. Nowitzke, E. Recknagel, J. Erxmeyer, A. Weidinger and J. I. Budnick, *Europhys. Lett., 15* (1991) 355.

9 J. Erxmeyer, G. Dortmann, J. Steiger, O. Boebel and A. Weidinger, *J. Less-Common Met., 172–174* (1991) 419.

10 L. Schlapbach (ed.), *Hydrogen in Intermetallic Compounds, Top. Appl. Phys., 63* (1988).

11 Y. Dalichaouch, M. S. Torikachvili, E. A. Early, B. W. Lee, C. L. Seaman, K. N. Yang, H. Zhou and M. B. Maple, *Solid State Commun., 65* (1988) 1001.
J. J. Neumeier, T. Bjornholm, M. B. Maple and I. K. Schuller, *Phys. Rev. Lett., 63* (1989) 2516.

12 M. Panzner, G. Keßler, M. Bobeth, A. Richter, S. Völlmar and W. Pompe, *Verh. Deutsche Physikalische Gesellschaft, 8* (1991) 1487.

13 A. Richter, M. Panzner, G. Keßler, A. Weidinger and J. Erxmeyer, *Proc. VDI Forum, Berlin, 1990*, Verein Deutscher Ingenieure, Düsseldorf, 1990, p. 421.

14 G. Keßler, A. Richter, M. Panzner, K. Teske, G. Irmer, A. Weidinger, J. Erxmeyer and H. Glückler, *Proc. VDI-Statusseminar Supraleitungs- und Tieftemperaturtechnik, Baden-Baden, 1991*, Verein Deutscher Ingenieure, Düsseldorf, 1991, p. 65.

15 E. V. Pechen, S. I. Krasnosvobodzev, G. Keßler, A. Richter, M. Panzner, O. Großmann and A. Teresiak, Preparation technique of ZrO_2 buffer layers for HTSC YBaCuO films on silicon by two-beam laser deposition, *Phys. Stat. Sol., 131* (1992) in the press.

16 N. Rüffer, C. H. Rüscher, J. Erxmeyer and K. Schulze, *Proc. VDI-Statusseminar Supraleitungs- und Tieftemperaturtechnik, Baden-Baden, 1991,* Verein Deutscher Ingenieure, Düsseldorf 1991, p. 127.

17 C. Thomsen, R. Liu, M. Bauer, A. Wittlin, L. Genzel, M. Cardona, E. Schönherr, W. Bauhofer and W. König, *Solid State Commun.*, *65* (1988) 55.

18 M. Stavola, D. M. Krol, L. F. Schneemeyer, S. A. Sunshine, J. V. Waszczak and S. G. Kosinski, *Phys. Rev. B*, *39* (1989) 287.

19 R. Feile, P. Leiderer, J. Kowalewski, W. Assmus, J. Schubert and U. Poppe, *J. Less-Common Met.*, *151* (1989) 125.

20 G. Burns, F. H. Dacol, C. Feild and F. Holtzberg, *Solid State Commun.*, *77* (1991) 367.

21 C. Thomsen, in M. Cardona and G. Güntherodt (eds.), *Light Scattering in Solids VI*, *Top. Appl. Phys.*, *68* (1991).

22 T. Siegrist, S. A. Sunshine, D. W. Murphy, R. J. Cava and S. M. Zahurak, *Phys. Rev. B*, *35* (1987) 7137.

23 Y. Liu, J. Y. Lee, M. J. Sumner, R. Sooryakumar and T. R. Lemberger, *Phys. Rev. B*, *42* (1990) 10090.